Available online at www.sciencedirect.com
ScienceDirect
Engineering Structures 30 (2008) 1745–1759
ENGINEERING STRUCTURES
www.elsevier.com/locate/engstruct

Reliability-based evaluation of steel structures using energy concepts

Eden Bojorquez[a,*], Sonia E. Ruiz[a], Amador Teran-Gilmore[b]

[a] *Instituto de Ingeniería, Universidad Nacional Autónoma de México, Apdo. Postal 70-472, Coyoacán, C.P. 04510, México, D.F., Mexico*
[b] *Universidad Autónoma Metropolitana, Depto. de Materiales, Av. San Pablo 180, Col. Reynosa Tamaulipas, 02200 México, D.F., Mexico*

Received 30 October 2006; received in revised form 26 October 2007; accepted 23 November 2007
Available online 21 February 2008

Abstract

A procedure for the structural assessment of the preliminary design of earthquake-resisting structures has been proposed. The reliability-based procedure takes into account explicitly the maximum and cumulative plastic deformation demands in the earthquake-resistant structure. Particularly, the procedure verifies that the structure has the capability to control and accommodate the maximum demands of global ductility, interstory drift and dissipated hysteretic energy (hysteretic energy dissipated through plastic deformation), through the use of: (A) Constant maximum ductility strength spectra and constant normalized dissipated hysteretic energy strength spectra with uniform annual failure rates; and (B) Transformation factors that take into account the differences between the response of multi-degree-of-freedom and single-degree-of-freedom systems. The use of the procedure, which is applicable to regular ductile steel frames that are designed according to the concepts of capacity design, is illustrated through its application to the structural revision of the preliminary design of an 8-story steel frame.

Keywords: Reliability-based evaluation procedure; Normalized dissipated hysteretic energy spectra; Uniform annual failure rate; Transformation factors

1. Introduction

As several structures designed according to modern seismic codes have not exhibited adequate dynamic behavior during major recent seismic events (e.g., Mexico 1985, Northridge 1994 and Kobe 1995), the international community of structural engineers is currently attempting to improve seismic design through the formulation of design methodologies that aim at damage control through displacement control [1–3]. This can be illustrated from the recommendations and conclusions derived from the ***International Symposium on Seismic Design Methodologies for the Next Generation of Codes*** [4], particularly the following one: "*The most suitable approach for seismic design to achieve the objectives of performance-based engineering appears to be deformation controlled design*." A large percentage of current seismic design codes are based on the use of pseudo-acceleration spectra to estimate the design lateral strength and lateral stiffness that the earthquake-resistant structure requires to control, within acceptable thresholds, its maximum lateral displacement demand.

In some cases, other parameters may be relevant to seismic performance. Particularly, experimental and field evidence suggests that severe cumulative plastic deformation demands can play an instrumental role in the structural safety of earthquake-resistant structures [5–8]. The superposition of the conclusions derived from the analytical and experimental research with the field evidence gathered after the 1985 Mexican Earthquakes consistently shows that structures subjected to the narrow-banded motions generated in the Lake Zone of Mexico City are likely to undergo severe plastic demands that if not accounted for during design can lead to unreliable performance [9–13]. Teran and Jirsa [14] observe that dissipated hysteretic energy demanded by narrow-banded motions can be three to four times larger than those corresponding to firm soil. As a consequence, they offer the following conclusion: "*displacement-control seismic design methodologies seem to provide adequate level of safety for the design of structures with stable hysteretic behavior and subjected to "typical" firm soil motions. Nevertheless, the use of low cycle fatigue models should be considered for the design of structures exhibiting rapid and excessive deterioration of*

* Corresponding author. Tel.: +52 5556233600 8478; fax: +52 5556233600 8050.
E-mail address: ebojorquezm@iingen.unam.mx (E. Bojorquez).

0141-0296/$ - see front matter © 2007 Elsevier Ltd. All rights reserved.
doi:10.1016/j.engstruct.2007.11.014

their hysteresis loop, and for any type of structure subjected to long-duration narrow-banded ground motion." Several similar studies carried out worldwide may help to understand why the following conclusion was reached during the ***International Symposium on Seismic Design Methodologies for the Next Generation of Codes*** [4]: "*Cumulative damage (dissipated energy) should be particularly considered in design for: Structures with rapidly deteriorating elements; long-duration ground motion*." Within this context, it is important to understand that several soft soil sites worldwide, such as the Bay Mud of the San Francisco Bay Area, have the potential to generate narrow-banded motions with very high energy contents [15].

Although there is no agreement on how energy demands should be accounted for during seismic design, the experimental and analytical evidence gathered so far indicates that structures can be protected from the effect of cumulative plastic demands by limiting their maximum deformation demand during an earthquake ground motion within a threshold that is significantly smaller than their ultimate deformation capacity under unidirectional loading [14,16–18]. In cases like these, seismic design should be updated to explicitly account for the effect of the cumulative plastic deformation demands, and thus, indirectly, for the effect of strong motion duration on structural performance [12,14,16,17,19,20]. This can be achieved through the use of damage indexes that explicitly consider the effect of the cumulative plastic deformation demands [5,10,14,21,22] or, alternatively, through the use of dissipated hysteretic energy spectra, as proposed herein.

One way to assess explicitly the effect of cumulative deformation demands on the level of structural damage is through energy concepts. The use of energy for this purpose was initially discussed by Housner [23]. Usually, energy-based methodologies are aimed to provide the structure with an energy dissipating capacity that is larger or equal than the expected energy demand [24,25]. Although some seismic design approaches have been based exclusively on the demand–supply balance of dissipated hysteretic energy [26,27], in some cases the explicit consideration of dissipated hysteretic energy during seismic design may lead to inadequate results because this approach does not consider the manner in which that the energy is dissipated. Thus, a better alternative for seismic design is to complement the use of dissipated hysteretic energy with other control requirements, such as those formulated by current seismic design formats (e.g., maximum ductility and interstory drift).

Other limitation of current seismic design is that it does not take explicitly into consideration the reliability of the earthquake-resistant structure. Besides that, most seismic regulations worldwide are based on studies carried out on single-degree-of-freedom (SDOF) systems having elasto-plastic behavior. In many cases of practical interest, these regulations do not guarantee a consistent exceedance level between the SDOF systems used to establish the design requirements, and the multi-degree-of-freedom (MDOF) structures designed according to them [28,29]. It should also be mentioned that design spectra contemplated by current codes are usually not associated to specific reliability levels or annual failure rates [30,31], and that degradation of the mechanical characteristics usually exhibited by structures that are not considered explicitly.

The aim of this paper is to introduce a reliability-based evaluation procedure for the assessment, from a structural point of view, of the preliminary design of steel frames. The evaluation is carried out within a scope in which the building has been preliminary designed according to a code format, and its seismic performance needs to be assessed before the design can be considered final. The acceptance conditions for the revision are based on those originally discussed by Collins et al. [32], which were extended by Rivera and Ruiz [33] to the design of structures having energy dissipating devices. The present study adds within this context, the effect of cumulative deformation demands through the use of constant normalized dissipated hysteretic energy strength spectra with uniform annual failure rates.

2. Basic definitions

2.1. Normalized dissipated hysteretic energy

The dissipated hysteretic energy can be defined from the equation of motion of a SDOF system:

$$m\,\ddot{x}(t) + c\,\dot{x}(t) + f_s(x,\dot{x}) = -m\ddot{x}_g(t) \tag{1}$$

where m is the mass of the system; c, the viscous damping coefficient; $f_s(x,\dot{x})$, the nonlinear force; $\ddot{x}$, the ground acceleration; and x, the displacement with respect to the base of the system. A dot above x indicates a derivative with respect to time. In the case of an elastic linear system, $f_s(x,\dot{x}) = k\,x$, where k is the stiffness of the system.

Integrating each member of Eq. (1) with respect to x, yields:

$$\int m\,\ddot{x}(t)\,\mathrm{d}x + \int c\,\dot{x}(t)\,\mathrm{d}x + \int f_s(x,\dot{x})\,\mathrm{d}x = -\int m\,\ddot{x}_g(t)\,\mathrm{d}x \tag{2}$$

Eq. (2) can be written as an energy balance equation [25]:

$$E_K + E_D + E_S + E_H = E_I \tag{3}$$

where E_K, E_D, E_S and E_H represent the kinetic (k), viscous damping (D), deformation (S) and dissipated hysteretic (H) energies, respectively; and E_I is the relative input energy. The term directly related to the cumulative plastic deformation demands is E_H.

The dissipated hysteretic energy E_H can be interpreted physically by considering that it is equal to the total area under all the hysteresis loops a structure undergoes during the ground motion. Although E_H provides a rough idea of the cumulative plastic deformations demands, this response parameter by itself does not provide enough information to assess the structural performance, in such a way that it is convenient to normalize it as follows:

$$E_N = \frac{E_H}{F_y \delta_y} \tag{4}$$

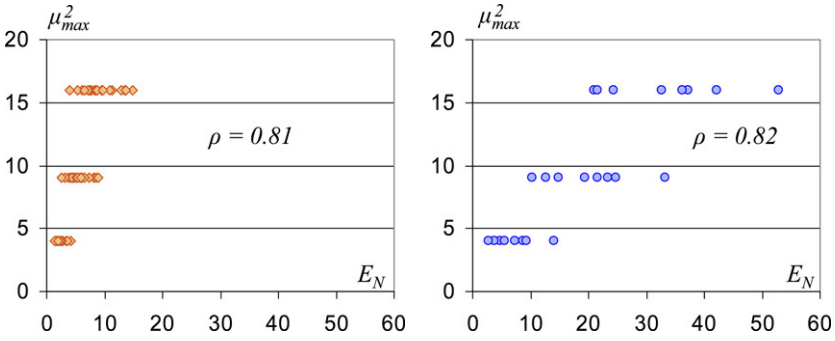

(a) LA, broad-banded motions. (b) Mexico soft, narrow-banded motions.

Fig. 1. Correlation between maximum ductility and normalized dissipated hysteretic energy.

where F_y and δ_y are the strength and displacement at first yield, respectively. For an elasto-perfectly-plastic system subjected to multiple plastic excursions, E_N is the sum of all plastic displacements reached in the different cycles normalized by δ_y, in such a way that E_N is a direct measure of the cumulative plastic deformation demands. For a system with degrading hysteretic behavior, E_N could be defined to include all plastic excursions for which the capacity does not degrade to a value less than a specified fraction of F_y (say 0.75). Such a definition allows for the rational evaluation of structural damage in degrading systems.

While several researchers have used E_N to develop recommendations for the design and detailing of ductile reinforced concrete elements [34–36], some design methodologies explicitly consider the effect of plastic cycling through energy concepts. Today there are still significantly different approaches towards the formulation of a design representation for the energy demands. Some researchers suggest that energy spectra can be formulated and used for design purposes [20,37–39]. Other options include accounting for cumulative loading in the structure through indirect measures of the plastic energy [16], and deriving the plastic energy demands from other relevant seismic demands [40].

An issue that needs to be considered carefully when formulating a design methodology that accounts for the effect of cumulative plastic deformations is the large correlation that exists between the dissipated hysteretic energy demand in structures, and other parameters that are currently used for their seismic design. For instance, the high levels of correlation observed by Teran and Jirsa [19] between the dissipated hysteretic energy demand on a structure and the strength reduction factor used during its seismic design lead them to conclude: "*if the strength reduction factor is defined in a transparent and reasonable manner within the code format, the energy content of the design ground motion is available for design purposes*."

Other relation that exhibits large values of correlation is that between the dissipated hysteretic energy and the maximum ductility demand. On the one hand, some researchers have considered that the large values observed for this correlation indicate that displacement-based procedures should be enough for seismic design (e.g., if the energy demands are closely correlated to maximum displacement demands, why should bother considering them explicitly). On the other hand, several researchers have taken advantage of this high correlation to formulate design methodologies that are based on the concept of target ductility [16,17,19,41]. To illustrate some of the issues that arise from the large correlation that exists between the energy demands and other relevant design parameters, Fig. 1 plots normalized dissipated hysteretic energy versus the square of the maximum ductility demand on the single-degree-of-freedom systems exhibiting elasto-perfectly-plastic behavior and 5% critical damping. The energy demands under consideration in the plot correspond to the mean E_N demands estimated in systems having a period ranging from 0.2 to 5 sec. Two sets of motions are considered, one of them corresponding to the Los Angeles (LA) urban area and one corresponding to Mexico City. The ground motions for LA, established for the FEMA/SAC Steel Project [42], were grouped in a set of twenty motions representative of the design earthquake for firm soil (broad-banded motions) with 10% exceedance in 50 years. The set of Mexican motions (*Mexico Soft*) was formed of seven narrow-banded long-duration ground motions recorded in the Lake Zone of Mexico City [19]. The *Mexico Soft* motions were scaled up in such a way that their peak ground velocity was equal to that corresponding to the EW component of the motion recorded at the *Secretaria de Comunicaciones y Transportes* during the 1985 Mexican Earthquake.

Although as pointed out in Fig. 1, a large correlation between the dissipated hysteretic energy demand and the square of the maximum ductility demand is observed, there is a significant difference in the dissipated hysteretic energy demands corresponding to the two sets of motions. In spite of the large correlation, energy demands cannot be characterized in a unique manner from the maximum displacement demand, in such a manner that seismic design cannot be formulated in similar terms for broad and narrow-banded motions. While Fajfar [16] has discussed the possibility of using the high correlation shown in Fig. 1 to estimate a reduced maximum displacement threshold that accounts for cumulative plastic deformation demands, several researchers have found that the conservatism usually associated to displacement-based formats is large enough to promote adequate seismic performance of ductile structures subjected to broad-banded motions. Nevertheless, Teran and Jirsa [14] suggest that the reduction in displacement thresholds due to the large energy demands

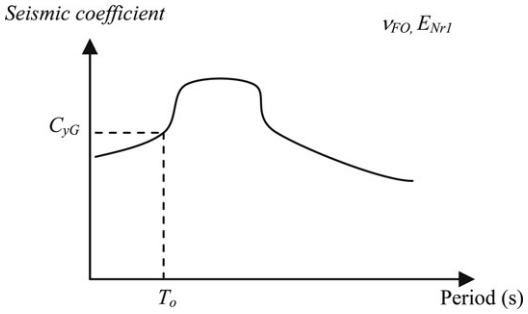

Fig. 2. Estimation of normalized hysteretic energy.

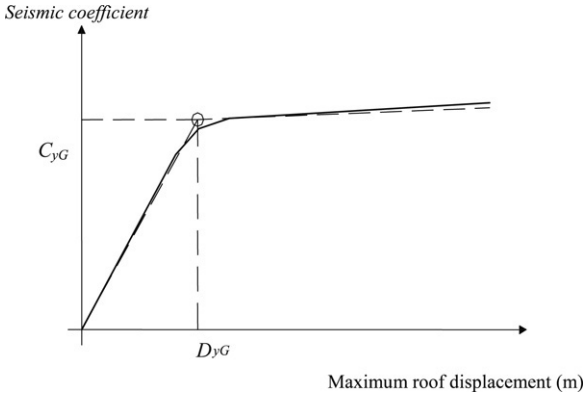

Fig. 3. Estimation of the actual seismic coefficient at yield.

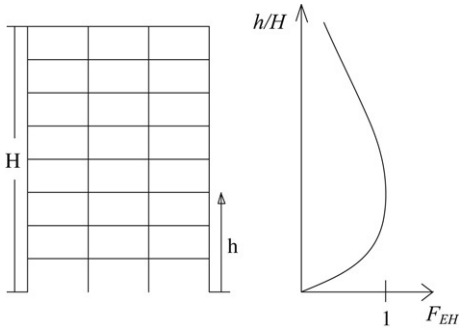

Fig. 4. Energy participation factor through height.

illustrated in Fig. 1(b) is large enough as to offset the conservatism associated to displacement-based approaches. Owing to this, several researchers have formulated energy-based methods that take into consideration reduced maximum displacement thresholds [16,17,19,41].

2.2. Normalized dissipated hysteretic energy spectrum with UAFR

A normalized dissipated hysteretic energy spectrum associated to particular values of E_N and of uniform annual failure rate (UAFR) is defined so that the lateral strength of a SDOF system with vibration period T is such that the system is able to control its normalized dissipated hysteretic energy demand (E_{Nr1}), within the threshold value of E_N, according to the annual failure rate associated to the spectra. As illustrated in Fig. 2, the ordinates of a normalized dissipated hysteretic energy spectrum correspond to strength (pseudo-acceleration, S_a). The algorithm to obtain a UAFR normalized dissipated hysteretic energy spectrum is similar to that used in obtaining a UAFR constant maximum ductility strength spectra, except that instead of controlling the maximum ductility demand, the former type of spectra focuses in controlling the cumulative ductility demand. Rivera and Ruiz [33] discuss in detail the formulation of UAFR constant maximum ductility strength spectra.

2.3. Normalized dissipated hysteretic energy capacity of the structure

In this study the normalized dissipated hysteretic energy capacity of a structure is defined as:

$$E_{\mathrm{NCG}} = \frac{E_{\mathrm{HG}}}{C_{yG} D_{yG} W} \tag{5}$$

where E_{HG} is the dissipated hysteretic energy capacity of the structure at the global level; D_{yG} and C_{yG}, the global displacement and global seismic coefficient at yield, respectively (see Fig. 3); and W, the total weight of the structure. The seismic coefficient is defined as the base shear of the structure normalized by W.

In order to evaluate the dissipated hysteretic energy structural capacity of a regular steel frame designed according to the principles of capacity design, the following simplifications can be considered [43]: (A) Plastic behavior tends to concentrate in its beams (the structure has been designed according to a strong column-weak beam approach; and (B) The level of energy dissipated in all the beams located at 1 story is similar. The dissipated hysteretic energy capacity of a frame can be approximated through the sum of the dissipated hysteretic energy capacity of all its beams. Nevertheless, not all the beams in a frame develop their full hysteretic energy dissipating capacity during the ground motion, in such a manner that it is necessary to consider the contribution of each beam. If, as stated before, the level of dissipated hysteretic energy in the beams of a story is similar, it is sufficient to consider the participation of each story to the global dissipated hysteretic energy mechanism. Herein, a story energy participation factor is used (F_{EH}). While Fig. 4 illustrates the concept, Appendix A discusses it in detail. Note that the maximum value for the participation factor is 1 for the stories that contribute with all their dissipated hysteretic energy capacity to the global capacity of the structure. According to the above, the dissipated hysteretic energy capacity of a frame can be established as:

$$E_{\mathrm{NCG}} = \frac{\sum_{i=1}^{NP} (E_{Hi} F_{\mathrm{EH}i})}{C_{yG} D_{yG} W} \tag{6}$$

where NP is the number of stories in the building; E_{Hi}, the dissipated hysteretic energy capacity of the ith story; and $F_{\mathrm{EH}i}$, its corresponding energy participation factor.

Evaluating the dissipated hysteretic energy capacity of structural elements in a rigorous way is a difficult task. In this study, the dissipated hysteretic energy capacity of steel

elements having a W section will be established as [26]:

$$E_{\mathrm{He}} = 2\,M_p\,\theta_{\mathrm{pa}} = 2\,Z_f\,F_y\theta_{\mathrm{pa}} \tag{7}$$

where Z_f is the section modulus of the flanges, F_y is the yield stress, and θ_{pa} is the cumulative plastic rotation capacity of the structural element.

Substituting Eq. (7) into Eq. (6):

$$E_{\mathrm{NCG}} = \frac{\sum_{i=1}^{NP}(2\,\mathrm{NC}\,Z_f F_y \theta_{\mathrm{pa}} F_{\mathrm{EH}i})}{C_{yG} D_{yG} W} \tag{8}$$

where *NC* is the number of bays in the frame.

3. Performance-based numerical seismic design

A numerical performance-based methodology requires that the response of the structural and nonstructural members be checked against threshold levels established as a function of the required seismic performance. Recently proposed design methodologies contemplate this check at three different steps:

(a) *Global Pre-design.* Quick and reasonable estimates of global seismic demands should be established and checked against global threshold levels. Within this context, the judicious use of response spectra provides information that allows the determination of a set of global mechanical characteristics (base shear, period of vibration, damping coefficient, and ultimate deformation capacity) that can adequately control and accommodate, within technical and cost constraints, the global response of the structure.
(b) *Preliminary Local Design.* Once the global mechanical characteristics have been determined, it is necessary to establish the structural properties and detailing at the local level. This step contemplates the analyses of complex analytical models of the structure, to obtain design information for the sizing, strength design and detailing of the structural elements.
(c) *Revision of the Preliminary Design.* Some recommendations have been formulated for the revision of the preliminary design through a series of dynamic structural analyses that address the global and local performance of the structure.

Within the context of performance-based design, the structural properties should be provided in such a way that, within technical and cost constraints, the structure is capable of controlling and accommodating adequately its dynamic response. Several authors have identified the importance of the *Global Pre-design and Preliminary Local Design*, and several methodologies have been offered to address these two steps [3, 41]. Krawinkler and Nassar [20] and Teran and Simon [39] have offered design methodologies that address these two steps and take into consideration the control of the maximum and cumulative displacement demands.

The evaluation procedure introduced herein focuses on the *Revision of the Preliminary Design* step. In this sense, the procedure is more an assessment tool than a design tool. As suggested before, the *Revision of the Preliminary Design* should consider the dynamic response of the structure, and check that this response does not exceed response thresholds established as a function of what is considered acceptable performance. To accomplish this, full-blown nonlinear time history analysis of the structure are required. Nevertheless, simple procedures have been established for structural assessment. For instance, the requirements included in FEMA 273 [44] evaluate the expected performance of the structure through combining a pushover analysis (nonlinear static analysis) and an estimate of the roof displacement of the structure derived from displacement spectra and a SDOF to MDOF transformation factor.

The procedure introduced herein follows a similar approach than the one contemplated by FEMA 273, in the sense that the evaluation approach is based on complementing a pushover analysis with estimates of the dynamic response of the structure derived from response spectra. Nevertheless, the proposed procedure does not only contemplate the maximum lateral displacement of the structure, but its maximum and cumulative plastic deformation demands and the reliability of the structure. To make this possible, the procedure contemplates two hazard curves; two different types of UAFR spectra (maximum ductility spectra and normalized dissipated hysteretic energy spectra); and three SDOF to MDOF transformation factors (one to check maximum ductility, one for maximum displacement, and one for dissipated hysteretic energy capacity). Given the limitations involved in obtaining in a reliable manner hazard curves and SDOF to MDOF transformation factors for irregular structures, it is suggested to limit the use of the proposed procedure to regular structures. An irregular structure will usually require full-blown nonlinear time-history analysis to evaluate its seismic performance.

4. Evaluation procedure

The evaluation procedure is based on the understanding that spectra can be used to capture the global dynamic response of MDOF structures. That is, it is assumed that through the use of spectra and appropriate SDOF to MDOF transformation factors, the dynamic response of a regular steel building can be estimated for structural assessment purposes. Particularly, spectra are used to revise whether: (A) The lateral strength of the structure is able to control the maximum global ductility demand within a threshold associated to an annual failure rate ν_{FO1}; (B) The lateral stiffness and strength can adequately control the maximum interstory drift demand within a threshold associated to an annual failure rate ν_{FO2}; and (C) The structure is able to control the normalized dissipated hysteretic energy demands within a threshold associated to an annual failure rate ν_{FO3}. For the sake of simplicity, it will be assumed that $\nu_{\mathrm{FO1}} = \nu_{\mathrm{FO2}} = \nu_{\mathrm{FO3}} = \nu_{\mathrm{FO}}$.

As with any other evaluation procedure, the procedure introduced herein may result in several iterations before it arrives to the final design of the structure. How much iteration depends on how the *Global Pre-design* and *Preliminary Local Design* steps have been carried out. While a well-conceived pre-design methodology should result in no iteration; a pre-design

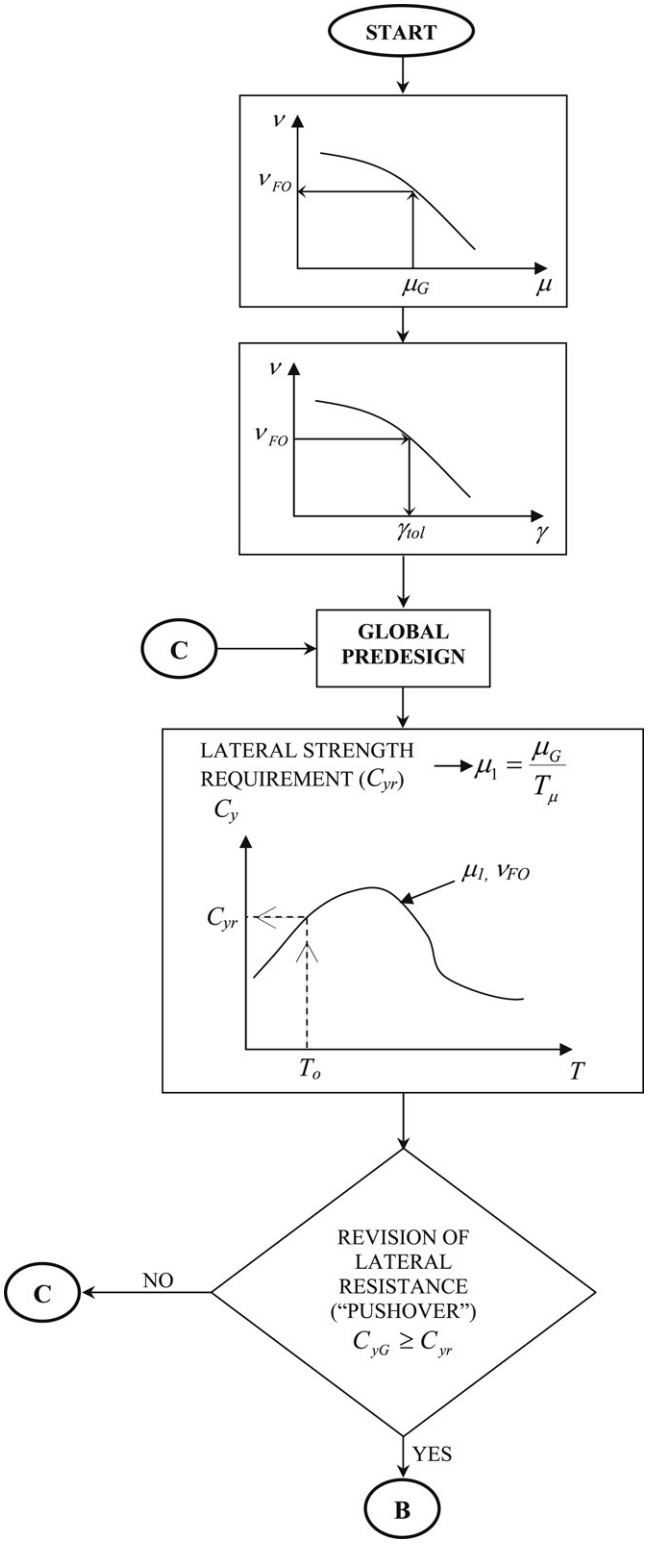

Fig. 5. Flowchart propose procedure.

that does not take into account explicitly the control of the maximum and cumulative deformation demands in the structure may result in one or more iterations.

The revision of the structural performance of the preliminary design for the life safety limit state implies the following (Fig. 5):

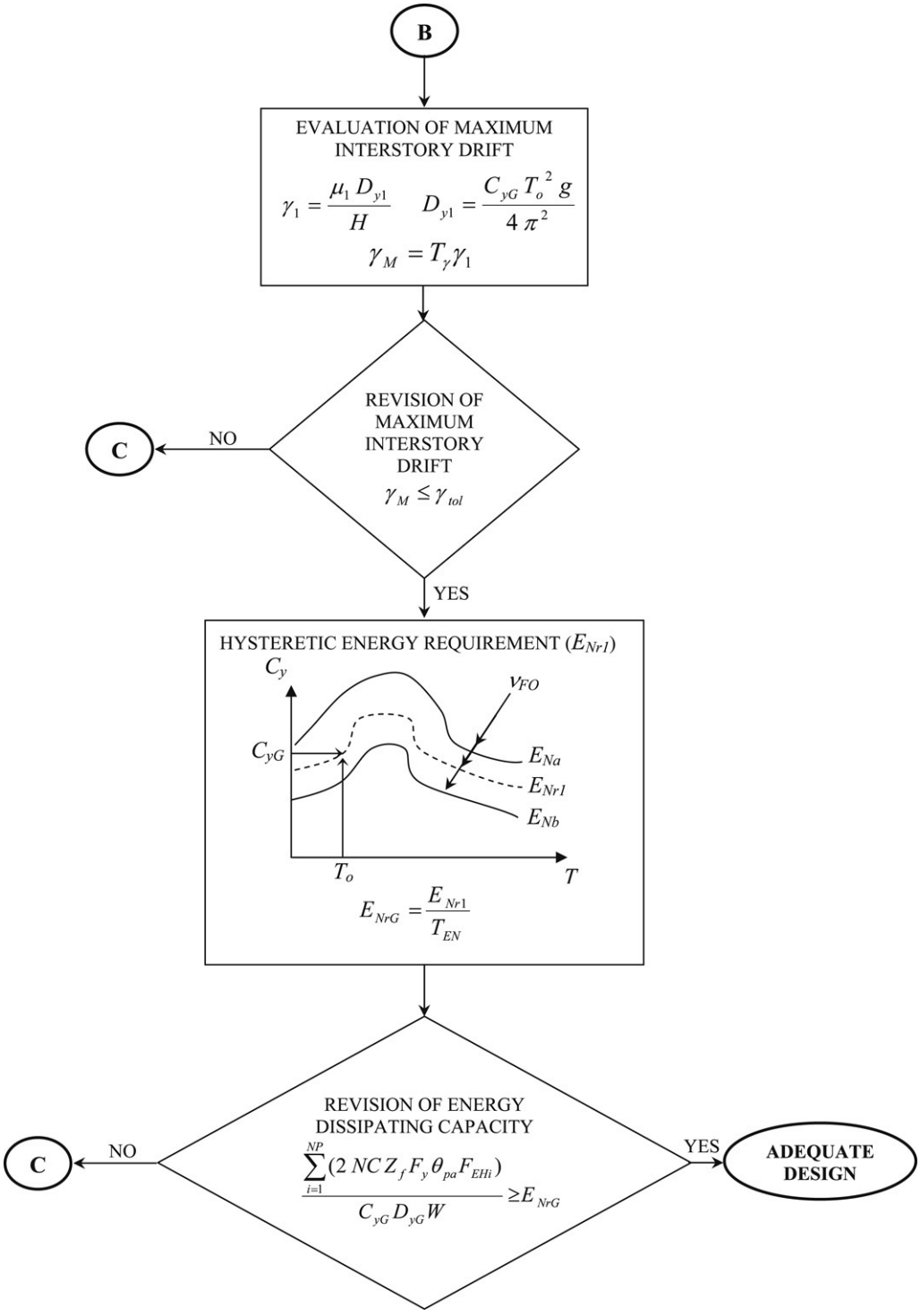

Fig. 5. (*continued*)

(a) *Desired annual failure rate.* The reliability associated to the structure is established in terms of annual failure rate. The first step is to establish the available global ductility capacity of the structure (μ_G), as a function of the detailing used for the structural elements and their connections. Then, the value of the annual failure rate associated to μ_G ($\nu_{FO1} =$ ν_{FO}) is established, as shown in Fig. 5, through a structure demand hazard curve. If the value of ν_{FO} is not acceptable, the value of μ_G could be modified through changes in the detailing used for structural elements and connections. Once the value of ν_{FO} is established, a second structure demand hazard curve is used as shown in Fig. 5 ($\nu_{FO2} =$

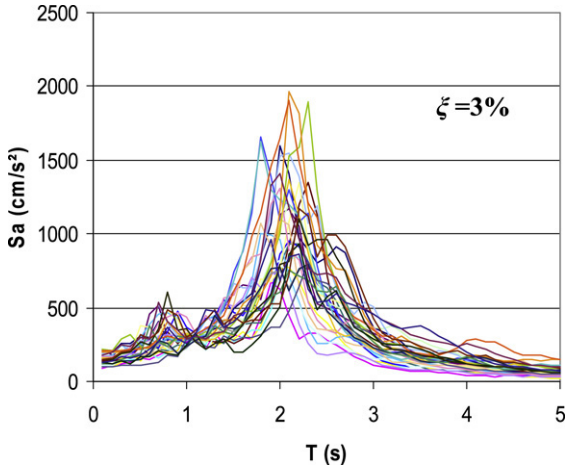

Fig. 6. Elastic response spectra for the ground motions under consideration.

ν_{FO}), to establish the value of the maximum tolerable interstory drift (γ_{tol}). Note that γ_{tol} could be critical for evaluation purposes, in which case the value of ν_{FO} should be established as a function of it.

(b) *Lateral strength requirements for maximum ductility control.* The global lateral strength requirements are evaluated from the design seismic coefficient (C_{yr}) established from a constant maximum ductility UAFR strength (pseudo-acceleration) spectrum. As shown in Fig. 5, the spectrum used for evaluation purposes (corresponding to a ductility μ_1 and a UAFR ν_{FO}) is evaluated at the actual period of the structure (To). To estimate the value of μ_1, a SDOF to MDOF transformation factor ($T_\mu = \mu_G/\mu_1$) is used. Appendix B discusses the obtention of T_μ and offers an expression (see Fig. B.2) to estimate its value for regular steel frames similar to that used to illustrate the application of the procedure. All spectra used in the illustrative example were derived from 31 ground motions recorded in the Lake Zone (subzone IIIb) of Mexico City. Detailed information of these motions is provided in Appendix A. Fig. 6 shows the elastic response spectra for the motions and 3% of critical damping. The motions under consideration were scaled according to Shome and Cornell [45]. Although several studies suggest that this scaling criterion is appropriate for broad-band motions [46,47], special care should be exercised when applying it to other soil conditions [48,49].

(c) *Revision of lateral resistance.* A "pushover" analysis is carried out to estimate the actual lateral strength in the structure, C_{yG} (see Fig. 3). The actual seismic coefficient in the structure is then compared against the required strength C_{yr}:

$$C_{yG} \geqslant C_{yr}. \tag{9}$$

In case Eq. (9) is not satisfied, the strength of the structural elements should be adjusted accordingly. In case it is satisfied, the procedure advances to the next step.

(d) *Revision of the maximum interstory drift.* As summarized in Fig. 5, the maximum interstory drift demand can be established through simplifying assumptions. First, the maximum drift in a SDOF model of the building can be estimated as:

$$\gamma_1 = \frac{\mu_1 D_{y1}}{H} \tag{10}$$

where μ_1 and D_{y1} are the expected ductility and yield displacement in the SDOF system, respectively; and H, the total height of the building. D_{y1} is estimated as:

$$D_{y1} = \frac{C_{yG} T_o^2 g}{4\pi^2}. \tag{11}$$

Next, the maximum interstory drift in the building (γ_M) can be estimated as:

$$\gamma_M = T_\gamma \gamma_1 \tag{12}$$

where T_γ is a drift transformation factor. Appendix B discusses the obtention of T_γ and offers an expression (see Fig. B.3) to estimate its value for regular steel frames similar to that used to illustrate the application of the procedure.

Finally, the estimated maximum interstory drift is checked, as shown in Fig. 5, against the design threshold, γ_{tol}:

$$\gamma_M \leqslant \gamma_{tol}. \tag{13}$$

If the value of γ_M does not satisfy Eq. (13), the structure must be resized (and if needed, its lateral strength adjusted). In case the equation is satisfied, the evaluation procedure advances to the next step.

(e) *Dissipated hysteretic energy requirements.* The expected cumulative plastic deformation demands are estimated from UAFR constant normalized dissipated hysteretic energy strength (pseudo-acceleration) spectra. Fig. 5 illustrates how the period To and the seismic coefficient C_{yG} are used to estimate the normalized dissipated hysteretic energy demands in an equivalent SDOF system (E_{Nr1}). Particularly, from a large set of constant normalized dissipated hysteretic energy strength spectra corresponding to different values of E_N, the spectrum that includes the coordinate pair defined by C_{yG} and To is selected, and its particular value of E_N assigned to the SDOF system. To estimate the dissipated hysteretic energy requirements in the actual structure, a normalized dissipated hysteretic energy transformation factor (T_{EN}) is used:

$$E_{NrG} = \frac{E_{Nr1}}{T_{EN}}. \tag{14}$$

Appendix B discusses the obtention of T_{EN} and offers an expression (see Fig. B.4) to estimate its value for regular steel frames similar to that used to illustrate the application of the procedure.

(f) *Revision of dissipated hysteretic energy capacity.* To satisfy the energy requirements in the structure, the following condition should be satisfied:

$$E_{NCG} \geqslant E_{NrG}. \tag{15}$$

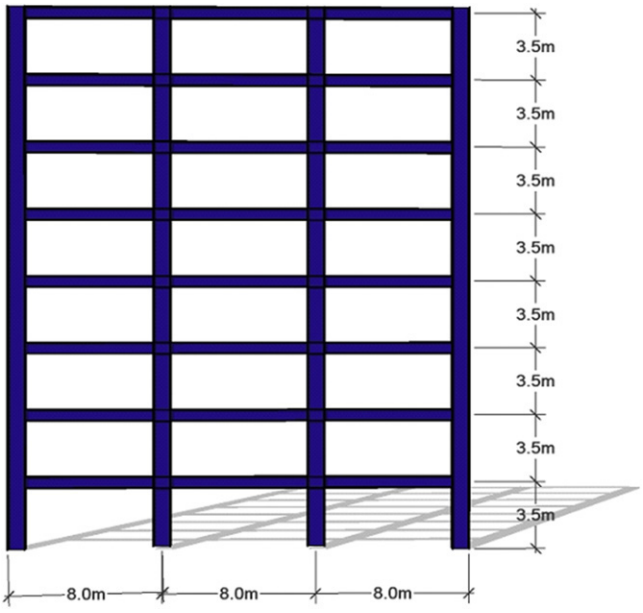

Fig. 7. Geometry of the structural frame.

Substituting Eq. (8) into Eq. (15), the following expression is obtained:

$$\frac{\sum_{i=1}^{NP}(2\,NC\,Z_f F_y \theta_{pa} F_{EHi})}{C_{yG} D_{y_G} W} \geqslant E_{NrG}. \quad (16)$$

In case the latter equation is not met, the detailing used in the structural elements and connections can be changed to increase their rotational capacities, or the lateral strength of the structure increased to reduce the normalized dissipated hysteretic energy demand.

Before concluding the description of the proposed procedure, it should be emphasized that the hazard curves should be site-specific. The hazard curves as well as the transformation factors should be established for specific types of buildings. Particularly the curves and factors used for the evaluation of a specific building should be derived for a number of stories, structural system and structural material that are consistent with the structural properties of that building. The hazard curves and transformation factors should be available to the designer, who should concentrate in applying them.

5. Illustrative example

The procedure is applied to refine the seismic design of a structural steel frame having 8 stories and 3 bays. The frame, shown in Fig. 7, is assumed to be located in the Lake Zone of Mexico City (specifically in subzone IIIb). The global pre-design of the frame is such that it complies with the requirements included in the Mexico City Building Code for ductile steel frames. While Table 1 summarizes the sizes of the structural elements of the frame (for all elements the yielding stress is 2533 kg/cm^2, which corresponds to A36 steel), an eigen-value analysis yields a fundamental period of vibration (T_o) of 1.07 s. The pre-design did not contemplate the reliability of the frame or its cumulative deformation demands.

Table 1
Sections proposed for the building

Story	Beams	Internal columns	External columns
1	$W24 \times 76$	$W36 \times 194$	$W36 \times 194$
2	$W24 \times 94$	$W36 \times 194$	$W36 \times 194$
3	$W24 \times 94$	$W36 \times 170$	$W36 \times 170$
4	$W24 \times 94$	$W36 \times 170$	$W36 \times 170$
5	$W24 \times 76$	$W36 \times 150$	$W36 \times 150$
6	$W21 \times 62$	$W36 \times 150$	$W36 \times 150$
7	$W21 \times 50$	$W36 \times 135$	$W36 \times 135$
8	$W21 \times 50$	$W36 \times 135$	$W36 \times 135$

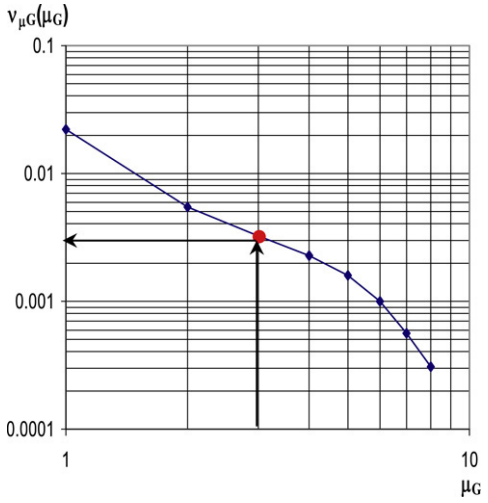

Fig. 8. Ductility hazard curve for a steel 8-story frame.

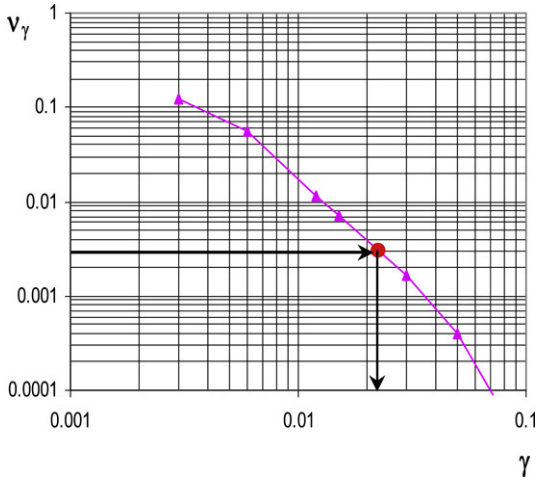

Fig. 9. Interstory hazard curve for a steel 8-story frame.

(a) *Desired annual failure rate.* As shown in Fig. 8, the example considers an annual failure rate ν_{FO} equal to 0.003, which is associated to a global ductility capacity μ_G of 3. This level of ductility is proposed through the consideration that a ductile steel frame should be able to reach this level of maximum plastic deformation. As shown in Fig. 9, a maximum tolerable interstory drift γ_{tol} of 0.023 is obtained for a ν_{FO} of 0.003.

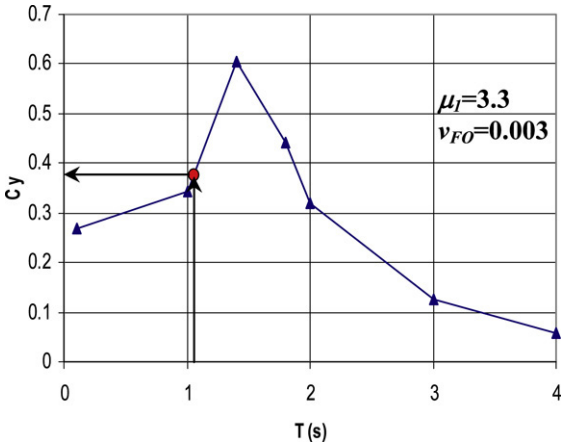

Fig. 10. Constant maximum ductility strength spectrum. Bilinear behavior with 3% post-yielding stiffness.

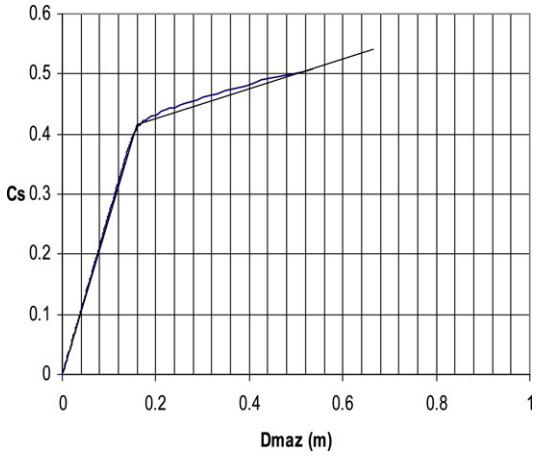

Fig. 11. Roof displacement vs seismic coefficient.

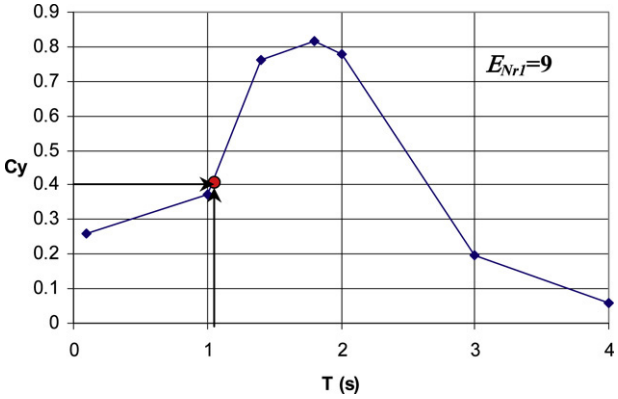

Fig. 12. Normalized hysteretic energy spectra associated to y_{FO} of 0.003.

(b) *Lateral strength requirements for maximum ductility control.* The required seismic coefficient for the frame is determined from a UAFR maximum ductility strength spectrum corresponding to ν_{FO} of 0.003. As shown in Fig. 10, a seismic coefficient $C_{yr} = 0.375$ is obtained for $To = 1.07$ s. According to Fig. B.2, T_μ equals 0.9, in such a manner that $\mu_1 = \mu_G / T_\mu = 3/0.9 = 3.3$.

(c) *Revision of lateral resistance.* The plot included in Fig. 11, derived from a "pushover" analysis of the frame, indicates that the seismic coefficient at yield is equal to 0.41. While the horizontal axis corresponds to roof displacement, the vertical axis plots the seismic coefficient. The preliminary design of the building satisfies the first acceptance condition: $C_{yG} \geqslant C_{yr}$ $(0.41 > 0.375)$, in such a way that the evaluation procedure proceeds to the next step.

(d) *Revision of the maximum interstory drift.* The revision of interstory drift demand in the building is established using Eqs. (10)–(12). According to Fig. B.3, T_γ equals 1.75, in such a manner that:

$$D_{y1} = \frac{C_{yG}\, T_o^2\, g}{4\,\pi^2} = 0.116\ m$$

$$\gamma_1 = \frac{\mu_1\, D_{y1}}{H} = 0.013$$

$$\gamma_M = T_\gamma \gamma_1 = 0.023.$$

The maximum expected demand of interstory drift is less or equal than the threshold established for γ_{tol} (=0.023) in such a way that the evaluation procedure proceeds to the next step.

(e) *Dissipated hysteretic energy requirements.*The dissipated hysteretic energy requirements are derived through normalized dissipated hysteretic energy strength spectra corresponding to $\nu_{FO} = 0.003$. Fig. 12 shows that $To = 1.07$ s and $C_{yG} = 0.41$ yield $E_{Nr1} = 9$. The normalized dissipated hysteretic energy required in the actual building is estimated by considering that Fig. B.4 yields T_{EN} equal to 3.5:

$$E_{NrG} = \frac{E_{Nr1}}{T_{EN}} = 2.6.$$

(f) *Revision of dissipated hysteretic energy capacity.* To satisfy the dissipated hysteretic energy requirements, the structure should satisfy:

$$\frac{\sum_{i=1}^{NP} (2\,NC\,Z_f\,F_y\,\theta_{pa}\,F_{EHi})}{C_{yG}\,D_{y_G}\,W} \geqslant 2.6 \tag{17}$$

where F_{EH} can be estimated as (see Appendix A):

$$F_{EH} = \text{mín}(F_{EH}*, 1) \tag{18}$$

where

$$F_{EH}* = \frac{1}{(-0.0675\mu + 2.82)\,h/H} \times \exp\left[-\frac{1}{2}\frac{(\ln(h/H) - \ln(0.031\mu + 0.3461))}{0.06\mu + 0.39}\right]$$

and h/H is the ratio of the height relative to the base at which the slab of a particular story is located and the total height of the building, and μ is the expected ductility demand in the structural frame. Considering for the example that $\theta_{pa} = 0.05$ and taking into consideration the properties summarized in Table 2, Eq. (17) yields:

$$\frac{76419}{0.41(0.15)(663600)} = 1.9 < 2.6. \tag{19}$$

Table 2
Summary of computations performed to establish the value corresponding to the left-hand side of Eq. (17)

Store	2 NC	F_y (kg/cm^2)	Z_f (cm^3)	θ_{pa}	Fp_{HE}	Σ (kg m)
1			2328		0.20	3538
2			3046		0.94	**21761**
3			3046		0.98	**22687**
4	6	2533	3046	0.05	0.69	**15974**
5			2328		0.42	**7431**
6			1692		0.24	**3086**
7			1161		0.14	**1236**
8			1161		0.08	**706**
Total						**76419**

As the above equation is not met, the details used in the structural elements and connections should be changed to increase their rotational capacities, or the lateral strength of the structure increased to reduce the normalized dissipated hysteretic energy demands. Considering an increment of θ_{pa} from 0.05 to 0.10, Eq. (17) yields:

$$\frac{2(76419)}{0.41(0.15)(663600)} = 3.8 > 2.6 \tag{20}$$

in such a manner that the design satisfies its evaluation objectives.

Before concluding the paper, the authors want to point out that the cumulative deformation demands are important for the seismic design of structures exhibiting low cumulative plastic deformation capacity, such as the one initially considered in the illustrative example ($\theta_{pa} = 0.05$); and for structures subjected to long-duration narrow-banded ground motions and exhibiting a fundamental period of vibration close to the dominant period of motion. For structures that do not fall in any of the two cases discussed above, conventional maximum displacement procedures should be used during their seismic evaluation.

6. Conclusions

A reliability-based seismic evaluation procedure for the preliminary seismic design of steel structures that accounts explicitly for energy demands was proposed. The procedure takes into account the reliability and the cumulative deformation demands in the structure through the use of normalized dissipated hysteretic energy spectra associated to a specific annual failure rate. The evaluation approach was applied to revise the preliminary design of an 8-story steel frame. It was observed that the demands of cumulative plastic deformation are important for structural frames with low cumulative rotational capacity. For structures with high plastic deformation capacity, it is usually sufficient to use a conventional evaluation criterion provided they are not subjected to long-duration narrow-banded ground motions and exhibit a fundamental period of vibration close to the dominant period of motion. Finally, it is concluded that the reliability-based seismic evaluation procedure proposed herein complement adequately current seismic design methodologies to achieve adequate performance of regular ductile steel frames in which energy demands are relevant to their seismic performance.

It is suggested to limit the use of the proposed procedure to regular steel frames designed according to the principles of capacity design. Owing to the use of a strong column-weak beam approach and of detailing that delays the occurrence of undesirable modes of behavior (such as local and lateral buckling), it is expected that in this type of buildings, plastic behavior is accommodated in a stable and even manner throughout their beams. An irregular structure will usually require full-blown nonlinear time-history analyses to assess its structural performance.

Acknowledgements

The support given by CONACYT to the first author is appreciated. This study was partially supported by DGAPA-UNAM (IN106205).

Appendix A. Dissipated hysteretic energy height distribution factor

The dissipated hysteretic energy demand is not usually constant through height. To take this into account, some researchers have proposed a linear distribution through height [26]. Nevertheless, recent studies suggest that if the energy dissipation is concentrated in the beams of a regular frame, a lognormal distribution represents best the manner in which the energy is dissipated through height [43]. A dissipated hysteretic energy participation factor (F_{EH}) is determined to estimate the contribution of each story to the energy dissipation capacity of a building. Particularly, F_{EH} evaluates the percentage of ultimate energy capacity that a story dissipates during the ground motion (the critical stories contribute their full energy dissipating capacity, fact that is indicated by $F_{EH} = 1$ for each one of those stories).

To establish F_{EH} for the frame considered in the illustrative example, eight regular structural steel frames were designed according to the Mexico City Building Code and subjected to 31 accelerograms recorded in subzone IIIb of the Lake Zone of Mexico City [50]. The buildings, which were assumed to be used for office space, exhibit three bays and a number of levels that range from 4 to 10 stories. The bay and interstory

Table A.1
Members sizes for the eight regular steel frames

Frame	I	II	III	IV	V	VI	VII	VIII
Number of Stories	4	4	6	6	8	8	10	10
Internal columns								
Story 1	$W21 \times 147$	$W21 \times 122$	$W30 \times 191$	$W30 \times 173$	$W36 \times 230$	$W36 \times 210$	$W36 \times 280$	$W36 \times 280$
Story 2	$W21 \times 147$	$W21 \times 122$	$W30 \times 191$	$W30 \times 173$	$W36 \times 230$	$W36 \times 210$	$W36 \times 280$	$W36 \times 280$
Story 3	$W21 \times 132$	$W21 \times 111$	$W30 \times 148$	$W30 \times 148$	$W36 \times 210$	$W36 \times 194$	$W36 \times 245$	$W36 \times 245$
Story 4	$W21 \times 132$	$W21 \times 111$	$W30 \times 148$	$W30 \times 148$	$W36 \times 210$	$W36 \times 194$	$W36 \times 245$	$W36 \times 245$
Story 5			$W30 \times 124$	$W30 \times 124$	$W36 \times 182$	$W36 \times 170$	$W36 \times 210$	$W36 \times 210$
Story 6			$W30 \times 124$	$W30 \times 124$	$W36 \times 182$	$W36 \times 170$	$W36 \times 210$	$W36 \times 210$
Story 7					$W36 \times 160$	$W36 \times 160$	$W36 \times 182$	$W36 \times 182$
Story 8					$W36 \times 160$	$W36 \times 160$	$W36 \times 182$	$W36 \times 182$
Story 9							$W36 \times 150$	$W36 \times 150$
Story 10							$W36 \times 150$	$W36 \times 150$
External columns								
Story 1	$W21 \times 111$	$W18 \times 97$	$W27 \times 178$	$W27 \times 146$	$W36 \times 210$	$W36 \times 194$	$W36 \times 280$	$W36 \times 280$
Story 2	$W21 \times 111$	$W18 \times 97$	$W27 \times 178$	$W27 \times 146$	$W36 \times 210$	$W36 \times 194$	$W36 \times 280$	$W36 \times 280$
Story 3	$W21 \times 93$	$W18 \times 86$	$W27 \times 146$	$W27 \times 129$	$W36 \times 182$	$W36 \times 182$	$W36 \times 245$	$W36 \times 245$
Story 4	$W21 \times 93$	$W18 \times 86$	$W27 \times 146$	$W27 \times 129$	$W36 \times 182$	$W36 \times 182$	$W36 \times 245$	$W36 \times 245$
Story 5			$W27 \times 114$	$W27 \times 114$	$W36 \times 160$	$W36 \times 160$	$W36 \times 210$	$W36 \times 210$
Story 6			$W27 \times 114$	$W27 \times 114$	$W36 \times 160$	$W36 \times 160$	$W36 \times 210$	$W36 \times 210$
Story 7					$W36 \times 135$	$W36 \times 135$	$W36 \times 182$	$W36 \times 182$
Story 8					$W36 \times 135$	$W36 \times 135$	$W36 \times 182$	$W36 \times 182$
Story 9							$W36 \times 150$	$W36 \times 150$
Story 10							$W36 \times 150$	$W36 \times 150$
Beams								
Story 1	$W16 \times 67$	$W16 \times 67$	$W18 \times 76$	$W18 \times 71$	$W21 \times 93$	$W21 \times 83$	$W21 \times 73$	$W21 \times 68$
Story 2	$W16 \times 57$	$W16 \times 57$	$W18 \times 76$	$W18 \times 76$	$W21 \times 101$	$W21 \times 93$	$W21 \times 101$	$W21 \times 93$
Story 3	$W16 \times 45$	$W16 \times 45$	$W18 \times 76$	$W18 \times 76$	$W21 \times 101$	$W21 \times 93$	$W21 \times 111$	$W21 \times 101$
Story 4	$W16 \times 40$	$W16 \times 40$	$W16 \times 67$	$W16 \times 67$	$W21 \times 93$	$W21 \times 83$	$W21 \times 111$	$W21 \times 101$
Story 5			$W16 \times 57$	$W16 \times 50$	$W18 \times 86$	$W18 \times 71$	$W21 \times 111$	$W21 \times 101$
Story 6			$W16 \times 50$	$W16 \times 45$	$W18 \times 76$	$W18 \times 65$	$W21 \times 101$	$W21 \times 93$
Story 7					$W18 \times 65$	$W18 \times 55$	$W21 \times 83$	$W21 \times 73$
Story 8					$W18 \times 50$	$W18 \times 46$	$W21 \times 73$	$W21 \times 68$
Story 9							$W21 \times 62$	$W21 \times 57$
Story 10							$W21 \times 57$	$W21 \times 50$

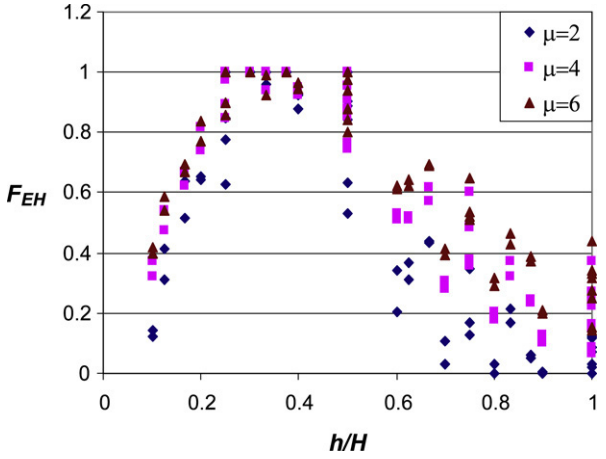

Fig. A.1. Mean values of the hysteretic energy participation factor (associated to a specific μ level) along the height obtained from the analysis of eight structural steel frames.

dimensions for the frames are those indicated in Fig. 7. Two versions of each frame were considered, one designed for standard detailing and the other for ductile detailing. A36 steel was used for the structural elements of the frames, whose dimensions are summarized in Table A.1. Some relevant characteristic for the ground motions are summarized in Table A.2. In the table, PGA and PGV denote the original peak ground acceleration and velocity, respectively, of the motions.

The records were scaled according to the criteria described in the paper. Fig. A.1 illustrates mean values of F_{EH} for the frames. h/H is the ratio between the height at which the slab of a particular story is located relative to the base (h), and the total height of the building (H). The distribution of F_{EH} along the height of the buildings is similar to a lognormal distribution function, in such a manner that the following expression is proposed:

$$F_{\mathrm{EH}} = \mathrm{mín}(F_{\mathrm{EH}}*, 1)$$

$$F_{\mathrm{EH}}* = \frac{1}{(-0.0675\mu + 2.82)\, h/H} \times \exp\left[-\frac{1}{2}\frac{(\ln(h/H) - \ln(0.031\mu + 0.3461))}{0.06\mu + 0.39}\right]. \quad \text{(A.1)}$$

Table A.2
Relevant characteristics of motions recorded in the lake zone of mexico city

Record	Date	Magnitude	Station	PGA (cm/s^2)	PGV (cm/s)
1	19/09/1985	8.1	SCT	178.0	59.5
2	21/09/1985	7.6	Tlahuac deportivo	48.7	14.6
3	25/04/1989	6.9	Alameda	45.0	15.6
4	25/04/1989	6.9	Garibaldi	68.0	21.5
5	25/04/1989	6.9	SCT	44.9	12.8
6	25/04/1989	6.9	Sector Popular	45.1	15.3
7	25/04/1989	6.9	Tlatelolco TL08	52.9	17.3
8	25/04/1989	6.9	Tlatelolco TL55	49.5	17.3
9	14/09/1995	7.3	Alameda	39.3	12.2
10	14/09/1995	7.3	Garibaldi	39.1	10.6
11	14/09/1995	7.3	Liconsa	30.1	9.62
12	14/09/1995	7.3	Plutarco Elías Calles	33.5	9.37
13	14/09/1995	7.3	Sector Popular	34.3	12.5
14	14/09/1995	7.3	Tlatelolco TL08	27.5	7.8
15	14/09/1995	7.3	Tlatelolco TL55	27.2	7.4
16	09/10/1995	7.5	Cibeles	14.4	4.6
17	09/10/1995	7.5	CU Juárez	15.8	5.1
18	09/10/1995	7.5	Centro urbano Presidente Juárez	15.7	4.8
19	09/10/1995	7.5	Córdoba	24.9	8.6
20	09/10/1995	7.5	Liverpool	17.6	6.3
21	09/10/1995	7.5	Plutarco Elías Calles	19.2	7.9
22	09/10/1995	7.5	Sector Popular	13.7	5.3
23	09/10/1995	7.5	Valle Gómez	17.9	7.18
24	11/01/1997	6.9	CU Juárez	16.2	5.9
25	11/01/1997	6.9	Centro urbano Presidente Juárez	16.3	5.5
26	11/01/1997	6.9	García Campillo	18.7	6.9
27	11/01/1997	6.9	Plutarco Elías Calles	22.2	8.6
28	11/01/1997	6.9	Est. # 10 Roma A	21.0	7.76
29	11/01/1997	6.9	Est. # 11 Roma B	20.4	7.1
30	11/01/1997	6.9	Tlatelolco TL08	16.0	7.2
31	11/01/1997	6.9	Tlatelolco TL55	13.4	6.5

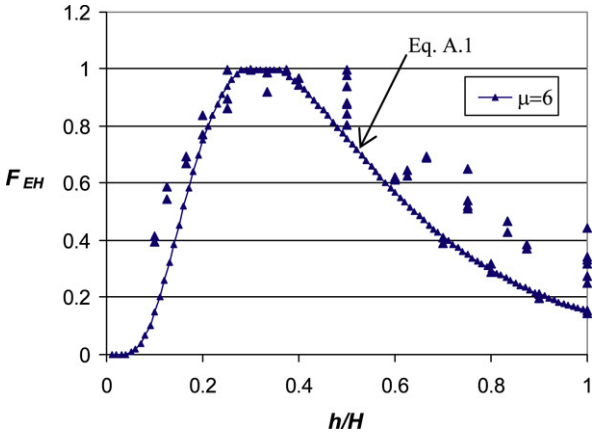

Fig. A.2. Comparison between FEH obtained from the analysis for $\mu = 6$ and with Eq. (A.1).

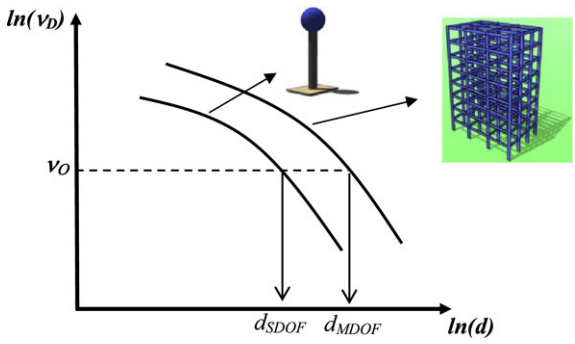

Fig. B.1. Outline of graphical procedure to determine the transformation factor for parameter d for the same annual rate.

Fig. A.2 compares the F_{EH} distribution estimated according to Eq. (A.1) with the actual distributions derived for the frames under consideration and a global ductility demand (μ) of 6. Similar comparisons were observed for other ductility values.

Appendix B. Transformation factors

Seismic design codes are commonly based on the use of spectra derived from SDOF systems. However, the ductility and other relevant parameters (e.g., maximum interstory drift and normalized dissipated hysteretic energy) in actual structures differ from those estimated through SDOF systems. As a consequence, it is desirable to consider the differences between the seismic demands in the MDOF structure and its SDOF model [51]. This can be achieved through the use of SDOF to MDOF transformation factors that can be derived according to what is illustrated in Fig. B.1.For the same level of annual failure rate, Figs. B.2–B.4 present transformation factors that relate ductility, maximum interstory drift, and normalized dissipated hysteretic energy demands developed in structural steel frames and their respective equivalent SDOF systems. The figures were developed from the response of eight steel frames

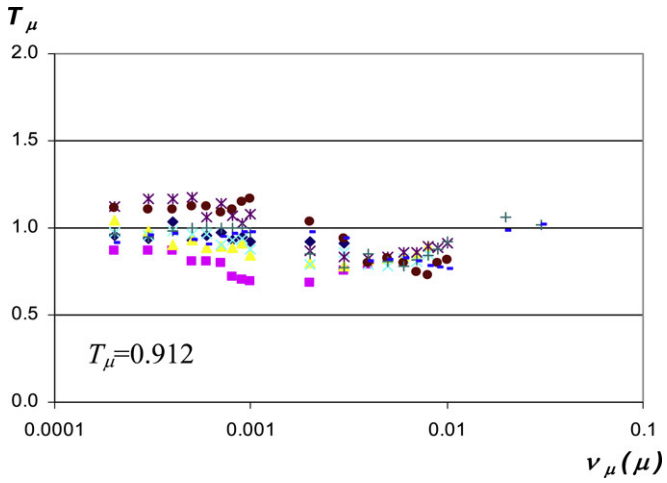

Fig. B.2. Ductility transformation factors.

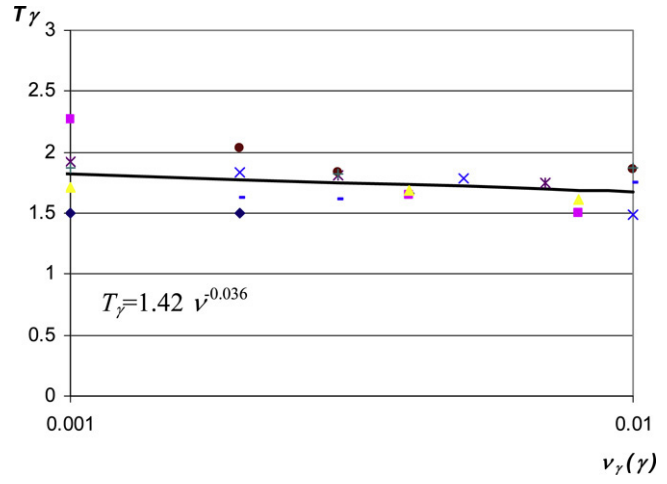

Fig. B.3. Maximum interstory drift transformation factors.

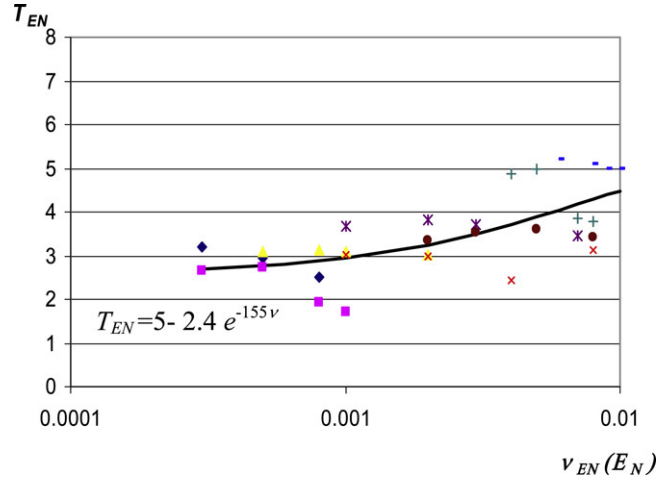

Fig. B.4. Normalized hysteretic energy transformation factors.

designed according to the Mexico City Building Code to different ground motions recorded in the Lake Zone of Mexico City [51]. Details of the frames and motions are offered in Appendix A. All transformation factors were established by normalizing the actual seismic demand in a structural steel frame by the respective demand estimated in an equivalent SDOF system. Equations to evaluate the transformation factors, which were obtained through a regression analysis that was based on the method of least squares, are offered in Figs. B.2–B.4. Low dispersion was observed for the three transformation factors. Particularly, mean values for the coefficients of variation for ductility, interstory drift and normalized dissipated hysteretic energy transformation factors are 0.12, 0.10 and 0.17, respectively. These low values of dispersion imply little uncertainty associated to the estimation of the factors.

References

[1] Moehle JP. Displacement based design of reinforced concrete structures subjected to earthquakes. Earthquake Spectra 1992;8(3):403–28.
[2] Priestley MJN. Myths and fallacies in earthquake engineering—conflicts between design and reality. Publication. American Concrete Institute; 1993. SP-157. p. 231–54.
[3] Priestley MJN. Performance based seismic design. In: 12° World conference on earthquake engineering (CD). 2000.
[4] Fajfar P, Krawinkler H. Conclusions and recommendations. In: Seismic design methodologies for the next generation of codes. A.A. Balkema; 1997.
[5] Park YJ, Ang AH. Mechanistic seismic damage model for reinforced concrete. ASCE Journal of Structural Engineering 1985;111(ST4): 740–57.
[6] Williams MS, Sexsmith RG. Seismic assessment of concrete bridges using inelastic damage analysis. Engineering Structures 1997;19(3):208–16.
[7] Stephens JE, Yao JTP. Damage assessment using response measurements. ASCE Journal of Structural Engineering 1987;113(4):787–801.
[8] Silva-Olivera H, Lopez-Batiz O. Estudio experimental sobre índices de daño en estructuras de concreto reforzado sujetas a cargas laterales. In: XIII Mexican conference on earthquake engineering. 2001 [in Spanish]. (CD).
[9] Teran-Gilmore A. Características mecánicas y desempeño sísmico de marcos dúctiles de concreto reforzado. In: XI Mexican conference on earthquake engineering. 1998 [in Spanish]. (CD).
[10] Rodriguez ME, Aristizabal JC. Evaluation of a seismic damage parameter. Earthquake Engineering and Structural Dynamics 1999;28:463–77.
[11] Huerta-Garnica B, Reinoso-Angulo E. Espectros de energía de movimientos fuertes registrados en México. Revista de Ingeniería Sísmica 2002;66:45–72 [in Spanish].
[12] Bojorquez E, Ruiz SE. Strength reduction factors for the valley of Mexico taking into account low cycle fatigue effects. In: 13° World conference on earthquake engineering (CD), paper 516, 2004.
[13] Arroyo D, Ordaz M. Demandas de energía plástica disipada en sistemas de un grado de libertad ubicados en suelos blandos. In: XV Mexican conference on earthquake engineering. 2006 [in Spanish]. (CD), Paper V-02.
[14] Teran-Gilmore A, Jirsa JO. A damage model for practical seismic design that accounts for low cycle fatigue. Earthquake Spectra 2005;21:803–32.
[15] Seed HB, Sun JI. Implications of site effects in the Mexico City Earthquake of Sept. 19, 1985 for earthquake-resistant design criteria in the San Francisco Bay Area of California. Report no.UCB/EERC-89/03. University of California at Berkeley; 1989.
[16] Fajfar P. Equivalent ductility factors taking into account low-cycle fatigue. Earthquake Engineering and Structural Dynamics 1992;21:837–48.
[17] Cosenza E, Manfredi G. Seismic design based on low cycle fatigue criteria. In: XI World conference on earthquake engineering (CD), paper 1141. 1996.
[18] Bertero VV. Performance-based seismic engineering: A critical review of proposed guidelines. In: Seismic design methodologies for the next generation of codes 1997. Bled, Slovenia, p. 1–31.

[19] Teran-Gilmore A, Jirsa JO. Energy demands for seismic design against low cycle fatigue. Earthquake Engineering and Structural Dynamics 2007; 36(3):383–404.
[20] Krawinkler H, Nassar A. Seismic design based on ductility and cumulative damage demands and capacities. In: Krawinkler H, Fajfar P, editors. Nonlinear Seismic Analysis and Design of Reinforced Concrete Buildings. UK: Elsevier Applied Science; 1992. p. 95–104.
[21] Krawinkler H, Zohrei M. Cumulative damage in steel structure subjected to earthquake ground motions. Computer and Structures 1983;16:531–41.
[22] Bozorgnia Y, Bertero V. Improved shaking and damage parameters for post-earthquake applications. In: Proceedings of the SMIP01 seminar on utilization of strong-motion data. 2001.
[23] Housner GW. Limit design of structures to resist earthquakes. In: First world conference on earthquake engineering. 1956.
[24] Akiyama H. Earthquake-resistant limit-state design for buildings. Tokyo: University of Tokyo Press; 1985.
[25] Uang CM, Bertero VV. Evaluation of seismic energy in structures. Earthquake Engineering and Structural Dynamics 1990;19:77–90.
[26] Akbas B, Shen J, Hao H. Energy Approach in performance-based design of steel moment resisting frames for basic safety objective. The Structural Design of Tall Buildings 2001;10:193–217.
[27] Choi H, Kim J. Energy-based seismic design of buckling-restrained braced frames using hysteretic energy spectrum. Engineering Structures 2006;28:304–11.
[28] Inoue T, Cornell CA. Seismic hazard analysis of MDOF structures, ICASP 6. Ciudad de México 1991;1;p.437–44.
[29] Esteva L, Ruiz S, Rivera J. Reliability and performance-based seismic design of structures with energy-dissipating devices. In: 9th World seminar on seismic isolation, energy dissipation and active vibration control of structures. 2005.
[30] Wen YK. Building Reliability and Code Calibration. Earthquake Spectra 1995;11:269–96.
[31] Cornell CA. Reliability-based earthquake-resistant design: the future. In: Proceedings, 11th World conference on earthquake engineering. Paper No. 2166.
[32] Collins KR, Wen YK, Foutch DA. Investigation of alternative seismic design procedures for standard building. Rep. no. UILU-ENG-95-2003. Urbana-Champaign: Illinois University.
[33] Rivera JL, Ruiz SE. Design approach based on UAFR spectra for structures with displacement-dependent dissipating elements. Earthquake Spectra 2007;23:417–39.
[34] Gosain NK, Brown RH, Jirsa JO. Shear requirements for load reversals on RC members. Journal of Structural Engineering 1977;103(ST7):1461–76.
[35] Scribner CF, Wight JK. Strength decay in R/C beams under load reversals. Journal of Structural Division. Proc. ASCE 1980;106(ST4):861–76.
[36] Darwin D, Nmai CK. Energy dissipation in RC beams under cyclic loading. Journal of Structural Engineering, ASCE 1985;112(8):1829–46.
[37] Akiyama H, Takahashi M. Response of reinforced concrete moment frames to strong earthquake ground motions. In: Krawinkler H, Fajfar P, editors. Nonlinear seismic analysis and design of reinforced concrete buildings. UK: Elsevier Applied Science; 1992. p. 105–14.
[38] Chou CC, Uang CM. Establishing absorbed energy spectra-an attenuation approach. Earthquake Engineering and Structural Dynamics 2000;29: 1441–55.
[39] Teran-Gilmore A, Simon R. Use of constant cumulative ductility spectra for performance-based seismic design of ductile frames. In: 8th US national conference on earthquake engineering (CD), Paper 1781. 2006.
[40] Decanini LD, Mollaioli F. An energy-based methodology for the assessment of seismic demand. Soil Dynamics and Earthquake Engineering 2001;21:113–37.
[41] Bertero RD, Bertero VV. Tall reinforced concrete buildings: Conceptual earthquake-resistant design methodology. Report no.UCB/EERC-92/16. University of California.
[42] Somerville PG, Smith N, Punyamurthula S, Sun J. Development of ground motion time histories for phase 2 of the FEMA/SAC Steel Project. Report SAC/BD-97/04, SAC Joint Venture.
[43] Bojorquez E, Diaz MA, Ruiz SE. Teran-Gilmore A. Correlation between local and global cyclic structural capacity of SMR frames. In: First European conference on earthquake engineering and seismology (CD). 2006.
[44] Federal Emergency Management Agency. NEHRP guidelines for the seismic rehabilitation of buildings. ASCE/FEMA 273 Prestandard.
[45] Shome N, Cornell CA. Probabilistic seismic demand analysis of nonlinear structures. Reliability of marine structures program 1999. Report no. RMS-35. Dept. of Civil Eng., Stanford University.
[46] Shome N, Bazurro P, Cornell CA, Carballo JE. Earthquakes, records and nonlinear MDOF responses. Earthquake Spectra 1998;14:469–500.
[47] Iervolino I, Cornell CA. Records selection for nonlinear seismic analysis of structures. Earthquake Spectra 2005;21(3):685–713.
[48] Baker J, Cornell CA. A vector-valued ground motion intensity measure consisting of spectral acceleration and epsilon. Earthquake Engineering and Structural Dynamics 2004;34:1193–217.
[49] Montiel MA, Ruiz SE. Influence of structural capacity uncertainty on seismic reliability of buildings under narrow-band motions. Earthquake Engineering and Structural Dynamics 2007;36:1915–34.
[50] Bojorquez E, Diaz MA, Ruiz SE, Garcia-Jarque F. Confiabilidad sísmica de varios edificios (cuatro a diez niveles) localizados en suelo blando de la ciudad de México, diseñados con el RCDF-2004. Revista de Ingeniería Sísmica 2007;76:1–27 [in Spanish].
[51] Bojorquez E, Ruiz SE. Factores de transformación de ductilidades, distorsiones máximas de entrepiso y de energía histerética normalizada entre S1GL y SMGL. In: Third national conference on earthquake engineering, CD [in Spanish].